Final NAG3-1968

Deterministic Multiaxial Creep and Creep Rupture Enhancements For CARES/Creep Integrated Design Code

By

Osama M. Jadaan

University of Wisconsin-Platteville, Platteville, WI 53818, USA

June 1998

Submitted to NASA Lewis Research Center

ABSTRACT

High temperature and long duration applications of monolithic ceramics can place their failure mode in the creep rupture regime. A previous model advanced by the authors described a methodology by which the creep rupture life of a loaded component can be predicted. That model was based on the life fraction damage accumulation rule in association with the modified Monkman-Grant creep rupture criterion. However, that model did not take into account the deteriorating state of the material due to creep damage (e.g., cavitaion) as time elapsed. In addition, the material creep parameters used in that life prediction methodology, were based on uniaxial creep curves displaying primary and secondary creep behavior, with no tertiary regime. The objective of this paper is to present a creep life prediction methodology based on a modified form of the Kachanov-Rabotnov continuum damage mechanics (CDM) theory. In this theory, the uniaxial creep rate is described in terms of stress, temperature, time, and the current state of material damage. This scalar damage state parameter is basically an abstract measure of the current state of material damage due to creep deformation. The damage rate is assumed to vary with stress, temperature, time, and the current state of damage itself. Multiaxial creep and creep rupture formulations of the CDM approach are presented in this paper. Parameter estimation methodologies based on nonlinear regression analysis are also described for both, isothermal constant stress states and anisothermal variable stress conditions This creep life prediction methodology was preliminarily added to the integrated design code CARES/Creep (Ceramics Analysis and Reliability Evaluation of Structures/Creep), which is a postprocessor program to commercially available finite element analysis (FEA) packages. Two examples, showing comparisons between experimental and predicted creep lives of ceramic specimens, are used to demonstrate the viability of this methodology and the CARES/Creep program.

ABSTRACT

High temperature and long duration applications of monolithic ceramics can place their failure mode in the creep rupture regime. A previous model advanced by the authors described a methodology by which the creep rupture life of a loaded component can be predicted. That model was based on the life fraction damage accumulation rule in association with the modified Monkman-Grant creep rupture criterion. However, that model did not take into account the deteriorating state of the material due to creep damage (e.g., cavitaion) as time elapsed. In addition, the material creep parameters used in that life prediction methodology, were based on uniaxial creep curves displaying primary and secondary creep behavior, with no tertiary regime. The objective of this paper is to present a creep life prediction methodology based on a modified form of the Kachanov-Rabotnov continuum damage mechanics (CDM) theory. In this theory, the uniaxial creep rate is described in terms of stress, temperature, time, and the current state of material damage. This scalar damage state parameter is basically an abstract measure of the current state of material damage due to creep deformation. The damage rate is assumed to vary with stress, temperature, time, and the current state of damage itself. Multiaxial creep and creep rupture formulations of the CDM approach are presented in this paper. Parameter estimation methodologies based on nonlinear regression analysis are also described for both, isothermal constant stress states and anisothermal variable stress conditions This creep life prediction methodology was preliminarily added to the integrated design code CARES/Creep (Ceramics Analysis and Reliability Evaluation of Structures/Creep), which is a postprocessor program to commercially available finite element analysis (FEA) packages. Two examples, showing comparisons between experimental and predicted creep lives of ceramic specimens, are used to demonstrate the viability of this methodology and the CARES/Creep program.

INTRDUCTION

Ceramic structural materials, such as silicon nitrides and silicon carbides, are continuously being developed and improved in response to demands for higher operating temperatures and load bearing capacity. Such demands are desirable for applications including gasoline, diesel, gas turbine engine components, and auxiliary power units. These systems are expected to survive for many thousands of hours, which necessitates subjecting them to low stress levels. The combination of high temperatures and low stresses typically causes failure for monolithic ceramics to be due to creep rupture (Wiederhorn, et al., 1994)

Two previous papers by the authors (Jadaan, et al., 1997, Powers, at al., 1996) described a deterministic damage based approach and the structure of an integrated design code, named CARES/Creep (Ceramics Analysis and Reliability Evaluation of Structures/Creep), to predict the lifetimes of structural components subjected to creep loading. This approach utilized commercially available FEA packages and took into account the effect of stress redistribution. In this approach the creep life of a component was descritized into short time steps, during which, the stress distribution is assumed constant. The damage, calculated using Robinson's linear damage rule (Robinson, 1952), was then computed for each time step based on a creep rupture criterion. The creep rupture models used in the code are the Monkman-Grant (Monkman, et al., 1956), and the modified Monkman-Grant (Menon, et al., 1994) criteria. Failure was assumed to occur when the normalized accumulated damage at any point in the component is greater than or equal to unity. The corresponding time would be the creep rupture life for the component.

The combination of the methodology described above, and the constitutive laws (Norton, and Baily-Norton) used to describe the material creep deformation behavior, have three shortcomings. The first shortcoming is with regards to the constitutive law. The Baily-Norton rule (Kraus, 1980, Norton, 1929, Boyle and Spence, 1983) relates the creep rate to stress, time and temperature in the primary and secondary regions of a typical creep curve. For ceramics that display no tertiary creep behavior, this rule was proven satisfactory for describing both the material's creep deformation behavior, and life prediction (Jadaan, et al., 1997, Powers, at al., 1996). However, some ceramics such as SN88 silicon nitride (French, et al., 1996, Luecke, et al., 1997), PY6 silicon nitride (Ferber, et al., 1992), and Si_3N4-$6Y_2O_3$-$2Al_2O_3$ (Todd, et al., 1989) do display tertiary creep behavior. For such materials, a more general constitutive creep law capable of describing the entire creep curve, including the tertiary creep regime, is necessary. Second, the linear damage summation approach in combination with the Monkman-Grant creep rupture criterion used to predict rupture in the methodology described above, did not take into account the instantaneous damaged state of the material as time elapsed. It assumes that a material loaded well into its creep design life displays the same creep characteristics as a virgin material. A more general and accurate approach, such as CDM, would incorporate the current damaged state of the material into the constitutive creep law. The third shortcoming of the methodology described above is due to the separation between the creep constitutive law (Baily-Norton) and the creep rupture criterion (Monkman-Grant). This could lead to reduced accuracy of life prediction due accumulated error induced by fitting (regressing) two separate sets of data. A more coherent theory, such as CDM which already incorporates the damaged state of the material into the constitutive law, would have both creep deformation and rupture embedded into one law.

Therefore, the objective of this paper is the development of a multiaxial creep life prediction methodology, based on a modified form of the continuum damage mechanics theory. This modified CDM based approach has the following advantages: 1) generalized capability of describing a given material's creep deformation behavior whether or not it displays a tertiary creep regime, 2) takes into account the effect of the current damaged state of the material on the deformation and rupture of the component through a scalar damage state variable, ω, and 3) the rupture criterion is incorporated directly into the creep constitutive law. This methodology utilizes commercially available FEA packages (ANSYS), and takes into account stress redistribution.

Similar to the main concept of life prediction described by the authors in their previous two papers, the creep life of a component is discretized into short time steps, during which, the stress and temperature distributions are assumed constant. Rupture life is determined using Robinson's linear damage summation rule (Robinson, 1952). Robinson's rule is the creep version of the Palmgren-Miner linear damage summation rule for fatigue (Miner, 1945). Namely, the damage is computed for each time step through dividing the time duration for that time step by the predicted rupture life based on the current stress/temperature state and CDM theory. The cumulative damage is subsequently calculated as time elapses and failure is assumed to occur when the normalized cumulative damage at any point in the component reaches unity.

BACKGROUND (UNIAXIAL STEADY STATE MODEL)

CDM has evolved into a mean to analyze the effect of damage accumulation on a component subjected to thermomechanical loading. A characteristic feature of CDM is the incorporation into the constitutive equations of one or more, scalar or tensorial, state (internal) variables as measures of the degradation of the material (Hault, 1987). What is meant by an internal damage variable, is that it can not be measured directly (Penny and Marriott, 1995). CDM, which is a phenomenological approach, can be thought of as a counterpart to fracture mechanics (FM). While FM deals with structures containing one or more cracks of finite size embedded in a non-deteriorating material, the aim of CDM is to predict the behavior of structures subject to material damage evolution (Hault, 1987).

One CDM model that stands out, is the phenomenological theory developed by Kachanov (1958, 1986) during the 1950s, and later expanded upon by Rabotnov (1969), Hayhurst (1975, 1984a, 1984b), Leckie (1977), Othman (1990), and Dunne (1990). This model contains one scalar damage parameter, ω, that describes the collective effect of deterioration in the material. It was developed to describe the process of brittle creep rupture in metals. At low loads, in metals, the deformation maybe small leading to essentially no variation in the cross sectional area with time. As time elapses, the material deteriorates as microcracks and cavities form. As these defects enlarge and ultimately coalesce, they would form macrocracks that lead to brittle failure. The aim of this paper is to reformulate this theory, proposed originally by Kachanov for metals, into a model that can be used with ceramics.

Kachanov elected to represent the damage via loss in material cross-section, due to cavitation. Consequently, the internal effective stress, σ, corresponding to a constant externally applied stress, σ_0, will increase with time as damage increases. He assumed that damage can be represented by a parameter he named the 'continuity', φ, which is defined as the ratio of the remaining effective area, A, to the original area, A_0. As damage accumulates, the resulting effective stress, σ, increases from its initial value σ_0 at time t=0, to a value $\sigma=\sigma_0 A_0/A$. Subsequently, Rabotnov replaced the continuity with the damage parameter, ω, such that $\omega = 1 - \varphi = 1- A/A_0$. This leads to the relationship between the effective stress, σ, and the applied stress, σ_0, being $\sigma=\sigma_0/(1-\omega)$. At t=0, $A=A_0$ and thus $\omega=0$. As time elapses, ω increases until it reaches a critical value ω_f, and failure occurs. Kachanov, Rabotnov, and Hayhurst and co-workers, dealing with creep of metals, assumed that $\omega_f=1$.

The damage rate, $\dot{\omega}$, is expressed in terms of the applied stress, σ_0, and the current state of damage, ω, as (Kachanov, 1986, Hayhurst, et al., 1974):

$$\dot{\omega} = C\,\sigma_0^{x}/(1-\omega)^{\phi} \qquad (1)$$

where C, x, and ϕ are material constants. Integrating equation 1 using the conditions that $\omega=0$ at t=0, and $\omega=1$ at $t=t_f$, where t_f if the uniaxial failure time, yields:

$$t_f = \sigma_0^{-x}/(C(1+\phi)) \qquad (2)$$

The instantaneous damage state, $\omega(t)$, can be derived to be:

$$\omega(t)=1-(1-t/t_f)^{1/(1+\phi)} \qquad (3)$$

For uniaxial stress states, Kachanov (1958) proposed a modified form of Norton's creep rate equation. In order to reflect the effect of the current state of damaged material on the creep rate, he replaced the applied stress σ_0 with the effective stress $\sigma=\sigma_0/(1-\omega)$, which resulted in the following steady state creep rate formula:

$$\dot{\varepsilon}_s = G\sigma^n = G(\sigma_0/(1-\omega))^n \qquad (4)$$

where G, and n are material parameters. Upon substituting equation 3 into equation 4 and integrating, the following two equivalent expressions for the creep strain, ε, are obtained:

$$\varepsilon(t)=G\sigma_0^n t_f \frac{1+\phi}{1+\phi-n}[1-(1-\frac{t}{t_f})^{\frac{1+\phi-n}{1+\phi}}] \qquad (5)$$

$$\varepsilon(t)=G\sigma_0^n t_f \frac{1+\phi}{1+\phi-n}[1-(1-\omega(t))^{1+\phi-n}] \qquad (6)$$

Figure 1 shows a schematic representation of a typical creep curve as described by the isothermal steady state constitutive equations 5 and 6 (Penny & Marriott, 1995). It is apparent from the curve that the steady state CDM model as described by Kachanov (1986) includes the features of tertiary creep following an initial minimum creep rate that remains essentially constant for the first 25% of life. At time zero when ω=0, equation 4 indicates that the steady state creep rate collapses to the Norton equation. As time elapses and the damage ω increases, the creep rate increases accordingly. Hence, due to the incorporation of the current damage state into the model, the steady state creep rate does not remain constant but rather tends to infinity as $t \rightarrow t_f$, and hence $\omega \rightarrow \omega_f$=1. According to Penny and Marriott (1995), and using the Kachanov model, most of the damage occurs later than 80% of life.

THEORY AND DAMAGE LAWS

Generalized Anisothermal Uniaxial Constitutive Model

The Kachanov model presented above was derived to describe the creep brittle rupture of metals, assuming isothermal steady state conditions. In addition, this model assumes that at failure a complete loss of integrity of the material occurs, which corresponds to ω_f=1. This condition results in the creep rate tending to infinity as $t \rightarrow t_f$.

In ceramics where tertiary creep behavior is observed, the creep rate increases as the failure time is approached but does not go to infinity. In addition, the assumption that a complete state of damage given by the condition that ω_f=1 is not observed experimentally in ceramics or even in many metals. Mennon, at al. (1994) observed that in a tensile silicon nitride NT-154 specimen tested at 1400 °C and failed at a strain of 2.5%, the ratio of cavitated area to the total area of the specimen was 5.5%. Penny and Marriott (1995) state that there are good reasons why ω at failure should be less than unity and devoted an appendix in there book to prove that point. Stamm and von Estorff (1992) who used ultrasonic techniques to determine cavity densities in steels concluded that the value of ω at failure is no where near unity, as was assumed by Kachanov. Hazime and White (1996) formulated a phenomenological damage model containing a hardening variable used to capture the continuous drop in creep rates with strain, observed in many ceramics. In there model they assumed that failure occurs when the damage reaches a critical value ω_f, which is predetrmined experimentally.

In this section, a generalized anisothermal CDM model that takes into account temperature variation and models the entire creep curve, including the primary and tertiary creep regions, will be derived. This model will take into account the effect of the current state of damage on the creep strain and strain rate accumulation. In addition, this model is generalized to capture the creep behavior of materials across the spectrum, starting with materials that display absolutely no tertiary creep characteristics, and ending with those showing severe tertiary behavior. Unlike the Hazime model, this generalized formulation does not require ω_f to be measured or known apriori, but rather is computed as a material parameter via nonlinear regression using standard creep data.

Primary creep can be taken into account by multiplying the damage rate and creep rate (equations 1 and 4) by the term t^m , where t is the time and m is a material parameter. Additionally, temperature dependence can be accounted for by multiplying equations 1 and 4 by an Arhenius type temperature formulation. Hence, the damage rate and creep rate can be described as:

$$\dot{\omega} = \frac{d\omega}{dt} = \frac{C\, t^{m}\, e^{-Q_D/RT}}{(1-\omega(t))^{\phi}} \sigma_0^{x} \qquad (7)$$

$$\dot{\varepsilon} = \frac{d\varepsilon}{dt} = G t^{m} e^{-Q_c/RT} \left(\frac{\sigma_0}{1-\omega(t)} \right)^{n} \qquad (8)$$

where C, x, m, ϕ, Q_D, G, n, and Q_c are material constants to be determined via nonlinear regression of creep data, R is the gas constant (8.31 J/mol.K), and T is the absolute temperature. The parameters Q_D and Qc represent the activation energies for damage and creep, respectively. The stress exponent, n, should be a positive number, while the time exponent, m, is generally negative.

Integrating equation 7, and using the conditions that at time zero, the damage ω=0, and that at the time of failure t_f, the damage reaches a critical value ω_f, results in the following formula for the time to failure:

$$t_f = \left\{ \frac{(1+m) e^{+Q_D/RT}}{C(1+\phi)\sigma_0^{x}} \left[1 - (1-\omega_f)^{1+\phi} \right] \right\}^{\frac{1}{1+m}} \qquad (9)$$

Equation 9 can be rewritten to obtain an expression describing ω_f in terms of stress, temperature, and the time to failure:

$$\omega_f = 1 - \left[1 - \frac{C(1+\phi) e^{-Q_D/RT}\, t_f^{1+m}}{(1+m)} \sigma_0^{x} \right]^{\frac{1}{1+\phi}} \qquad (10)$$

A function describing the current state of damage as a function of time, ω(t), can be derived by integrating equation 7, or by substituting t for t_f in equation 10:

$$\omega(t) = 1 - \left[1 - \frac{C(1+\phi) e^{-Q_D/RT}\, t^{1+m}}{(1+m)} \sigma_0^{x} \right]^{\frac{1}{1+\phi}} \qquad (11)$$

Another useful expression for the current state of damage, can be derived by combining equations 9 and 11:

$$\omega(t) = 1 - \left\{ 1 - \left(\frac{t}{t_f} \right)^{1+m} \left[1 - (1-\omega_f)^{1+\phi} \right] \right\}^{\frac{1}{1+\phi}} \qquad (12)$$

Now that the damage evolution has been derived, we will turn our attention to the creep strain accumulation and the effect of the current state of damage on it. The creep rate expression was given earlier through equation 8. Substituting equation 12 into equation 8 yields the following alternative expression for the creep rate:

$$\dot{\varepsilon}=Gt^{m}\,\sigma_0^{n}\,e^{-Q_c/RT}\left\{1-\left(\frac{t}{t_f}\right)^{1+m}\left[1-\left(1-\omega_f\right)^{1+\phi}\right]\right\}^{\frac{-n}{1+\phi}} \qquad (13)$$

Finally, upon integration of equation 13, an expression describing how the creep strain varies with time, temperature, and stress is derived:

$$\varepsilon(t)=\frac{Gt_f^{1+m}\,\sigma_0^{n}\,e^{-Q_c/RT}}{(1+m)\left(\frac{1+\phi-n}{1+\phi}\right)\left[1-\left(1-\omega_f\right)^{1+\phi}\right]}\left\{1-\left[1-\left(\frac{t}{t_f}\right)^{1+m}\left[1-\left(1-\omega_f\right)^{1+\phi}\right]\right]^{\frac{1+\phi-n}{1+\phi}}\right\} \qquad (14)$$

Equation 14 describes the entire creep curve, including the primary, secondary, and tertiary regions. Depending on the value for ω_f, equation 14 can simulate creep curves with severe tertiary behavior ($\omega_f \rightarrow 1$) as well as creep curves displaying no tertiary characteristics ($\omega_f \rightarrow 0$). This behavior can be visualized by setting $\omega=\omega_f$ in the creep rate equation 8, which results in formulation for the creep rate at failure. The creep strain Equation 14 can be rewritten in terms of the current state of damage $\omega(t)$ as follows:

$$\varepsilon(t)=\frac{Gt_f^{1+m}\,\sigma_0^{n}\,e^{-Q_c/RT}}{(1+m)\left(\frac{1+\phi-n}{1+\phi}\right)\left[1-\left(1-\omega_f\right)^{1+\phi}\right]}\left\{1-\left[1-\omega(t)\right]^{1+\phi-n}\right\} \qquad (15)$$

An expression for the rupture strain, ε_f, can be obtained by setting $\omega=\omega_f$ in equation 15:

$$\varepsilon_f=\frac{G\sigma_0^{n}\,t_f^{1+m}\,e^{-Q_c/RT}}{(1+m)\left(\frac{1+\phi-n}{1+\phi}\right)\left[1-\left(1-\omega_f\right)^{1+\phi}\right]}\left\{1-\left[1-\omega_f\right]^{1+\phi-n}\right\} \qquad (16)$$

Note that all the equations derived in this section will collapse to Kachanov's isothermal steady state formulation if the activation energies and the time exponent parameters (Q_D, Q_c, m), are set to zero, and $\omega_f=1$.

A worthwhile discussion at this point is one that relates the damage accumulation using the Robinson's (1952) time fraction rule, D, and the CDM current state of damage, ω. This is necessary because under conditions of varying temperature and/or stress conditions, the Robinson's linear damage summation rule is utilized to predict creep rupture. In order to accomplish this task of comparing these two formulations, let us first rewrite equation 12 into the following form:

$$D = \frac{t}{t_f} = \left[\frac{1-(1-\omega)^{1+\phi}}{1-(1-\omega_f)^{1+\phi}}\right]^{\frac{1}{1+m}} \qquad (17)$$

The term D represents the damage due to creep deformation after time t and is given by the time fraction t/t_f. For conditions in which constant uniaxial stress states exit, it can be seen that at the time of failure, when $\omega=\omega_f$ and $t=t_f$, D=1. It is also apparent from equation 17 that the damage as defined by the life fraction term, t/tf, does not equal the current state of damage, ω, except at the two extremities of time zero and rupture time. Hence, for constant stress and temperature conditions, either one of the two damage terms can be used to predict rupture since they both converge to unity at failure.

However, for varying stress (stress relaxation) and/or temperature conditions, the linear damage summation rule should be utilized. For such conditions, the design life of the component is discritized into short time steps. the damage is computed for each time step through dividing the time duration for that time step, t_i, by the predicted rupture life, t_{fi}, based on the current stress and temperature states and CDM theory (equation 9). The cumulative damage, $D = \Sigma D_i = \Sigma(t_i/t_{fi})$, is subsequently calculated as time. Failure is assumed to occur when the normalized cumulative damage, D, at any point in the component reaches unity.

Other forms of creep damage assessment have recently been suggested, One such formulation is based on the concept of ductility exhaustion (Zamrik and Davis, 1990, Hales, 1988)). Ductility exhaustion is similar in concept to Robinson's life fraction rule except that it uses strain fraction. Failure occurs when the cumulative strain reaches a critical value, usually assumed equal to the ductility in a constant load creep test (Penny and Marriott, 1995). Hence, the condition for failure is $D=\Sigma(\varepsilon_i/\varepsilon_{fi})=1$.

Multiaxial Stress Formulation

Engineering structures are seldom subjected to uniaxial stress states. Hence, it is necessary to extend the unixial CDM formulation presented in the previous section to the multiaxial case. CDM Multiaxial stress development for isothermal steady state conditions, and assuming that $\omega_f = 1$ at failure, have been described by Kachanov (1958), Leckie and Hayhurst (1977), Hayhurst et al. (1983, 1984), Penny and Marriott (1995), and Krajcinovic (1987).

The uniaxial creep and damage laws were given through equations 8 and 7, respectively. In the absence of damage the multiaxial creep rate equation is usually stated in the Von Mises form. A similar creep rate law taking into account the effect of damage can be stated as:

$$\dot{\varepsilon}_{ij} = \frac{d\varepsilon_{ij}}{dt} = \frac{3}{2}\frac{\dot{\varepsilon}_e}{\sigma_e}S_{ij} = \frac{3}{2}\frac{G t^m e^{-Q_c/RT}\sigma_e^{n-1}}{(1-\omega(t))^n}S_{ij} \qquad (18)$$

where $d\varepsilon_{ij}/dt$ is the creep strain rate tensor, S_{ij} is the deviatoric stress tensor, ε_e is the effective creep strain, and σ_e is the Von Mises effective stress. The effective creep rate is obtained by replacing the uniaxial stress with the effective stress in equation 8. Similarly, the damage law for the multiaxial stress condition can be written as (note that the damage is a scalar term):

$$\dot{\omega} = \frac{d\omega}{dt} = \frac{C t^m e^{-Q_D/RT}}{(1-\omega(t))^\phi}\sigma_{eq}^x \qquad (19)$$

where σ_{eq} is the equivalent stress. Integrating equation 19, and assuming that σ_{eq} remains constant, yields the following equation describing the current state of damage in a multiaxial stress state:

$$\omega(t)=1-\left[1-\frac{C(1+\phi)e^{-Q_D/RT}\ t^{1+m}}{(1+m)}\sigma_{eq}^{x}\right]^{\frac{1}{1+\phi}} \qquad (20)$$

Solving for the rupture time using equation 20 by setting $\omega=\omega_f$ (this corresponds to $t=t_f$), results in:

$$t_f=\left\{\frac{(1+m)e^{Q_D/RT}}{C(1+\phi)\sigma_{eq}^{x}}\left[1-(1-\omega_f)^{1+\phi}\right]\right\}^{\frac{1}{1+m}} \qquad (21)$$

The equivalent stress term, σ_{eq}, correlates the damage under uniaxial tension with the damage under multiaxial stress states. Kachanov (1958) proposed setting the equivalent stress equal to the maximum normal tensile stress, σ_1 ($\sigma_{eq}=\sigma_1$). Hayhurst, on the otherhand, proposed the following mixed criteria for the equivalent stress:

$$\sigma_{eq}=\alpha\sigma_1+(1-\alpha)\sigma_e \qquad (22)$$

Where α is a factor to be determined from two sets of creep tests, each carried out under a different multiaxial stress state (Hayhurst, et al, 1984). Two extreme material classifications can be seen through equation 22. The first category corresponds to material failure governed by the maximum principal tensile stress criterion ($\alpha=1$); the behavior of copper is described by this criterion. For the second category, the creep rupture time is governed by maximum effective (Von Mises) stress criterion ($\alpha=0$); the behavior of aluminum is described by this criterion. Unfortunately, for ceramics no comprehensive multiaxial creep database exists. Thus, in this paper the equivalent stress will be set to either σ_1 or σ_e whichever results in the shorter life to failure.

In our life prediction methodology, FEA is used perform the stress and creep deformation analysis. The ANSYS FEA package was utilized for this purpose. The ANSYS program allows the user to define his/her creep constitutive law through its user defined creep subroutine. This capability was used and described in more detail by the authors (Jadaan, et al., 1997) in a previous publication. The CDM creep rate and damage laws (equations 18, 20, and 22) were programmed into ANSYS to compute the creep strain rate tensor, and consequently the stress and deformation history for the component in question.

The CARES/Creep code developed by the authors (Powers, et al., 1996, Jadaan, et al., 1997) to predict the creep rupture life of ceramic components based on the modified Monkman-Grant creep rupture criterion, was expanded to add the capability of predicting rupture based on CDM. In summary, the CARES/Creep code is made up of two modules and is currently customized to run as a post-processor to the ANSYS FEA code. The first module is a parameter estimation program used to compute the creep material parameters. Parameter estimation for the CDM laws will be discussed in the next section. The second module contains the coding for calculating the cumulative damage as a function of time at each node/element of the meshed component, and thus its creep rupture life. The methodology used in this module is described next.

As was stated earlier, to carryout a creep life prediction analysis for a given component, the creep life of the component is divided into short time steps, t_i, during which the stress state is assumed constant. This is done because even for constant load/temperature conditions, the stress state can vary with time due to creep deformation. During each time step and at each node/element, the time to failure, t_{fi}, is calculated using equation 21 and the existing stress/temperature state. Subsequently, the damage for each time step and at each node/element based on Robinson's time fraction rule, $D_i = t_i/t_{fi}$, is computed. Damage summation as a function of time, $D = \Sigma D_i = \Sigma(t_i/t_{fi})$, is then performed at each node/element. Failure commences when the damage, D, at any node/element reaches unity.

PARAMETER ESTIMATION

The CDM model presented in this paper contains nine material parameters to be determined form creep tensile data. These parameters are G, n, m, ϕ, Q_c, ω_f, C, x, and Q_D. Due to the nonlinear nature of the model, nonlinear regression using, the IMSL routine DRNLIN, was used to compute these constants. This routine utilizes a modified Levenberg-Marquardt (Press, et al., 1989) least squares method.

The IMSL nonlinear regression routine requires the user to provide initial guesses for the parameters to be determined. The routine would then use these guesses as starting values and search in the space surrounding them for optimized parameters that would minimize the sum of square errors (SSE). Due to the large number of parameters to be determined in this model, the routine often did not converge. For the trials when the IMSL routine converged, it often converged to a local minimum, yielding values close to what was initially guessed or values that did not make physical sense such as zero activation energies or negative stress exponents. This dependence of converged parameter values on the initial guesses cause two problems. The first is that different users making different initial guesses can have different creep parameters. This will result in different life predictions for the same component. The second problem is that the accuracy of the computed parameters depends on the quality of the initial guesses made.

In order to alleviate these problems, and to automate the nonlinear regression parameter estimation procedure in such a way that all users would converge to the same parameters, the following parameter estimation methodology was devised:

1) Use the Baily-Norton constitutive creep model to obtain initial guesses for the four CDM creep parameters, G, n, m, and Q_c. The Baily-Norton model is a relatively simple one, which parameters can be obtained via simple multiple linear regression analysis. The Baily-Norton creep rate equation is given by:

$$\dot{\varepsilon}=C_1\,\sigma_0^{C_2}\,t^{C_3}\,e^{-C_4/T} \qquad (23)$$

where C_1 through C_4, are material constants that can be determined via multiple linear regression analysis. The parameter estimation module within CARES/Creep is used to compute these parameters (Powers, et al., 1996, Jadaan, et al., 1997).

Comparing the CDM and the Baily-Norton creep rate equations 8 and 23, it can be seen that the parameters G, n, m, and Qc/R have the same correspondence and physical interpretation as the Baily-Norton parameters, C_1, C_2, C_3, and C_4, respectively. Therefore, these C_1 through C_4 parameters are used as good initial guesses for the four CDM parameters, G, n, m, and Q_c/R, respectively.

2) From equations 14 and 15, it is apparent that ϕ should be greater than n-1, in order to obtain positive tensile strains in response to positive tensile stresses. In order to automate the parameter estimation process, the initial guess for ϕ is set randomly equal to n+2. The critical damage state parameter must remain within the range $0 < \omega_f \leq 1$. Again, in order to automate the process, ω_f is set equal to 0.1 for materials displaying very little or no tertiary creep behavior, and 0.9 for materials displaying significant tertiary creep behavior. Another alternative available to the user is to set ω_f to a default intermediate value of 0.5, and let the nonlinear regression routine shift it up or down depending on whether or not the creep data displays tertiary creep characteristics.

Now that we have good starting guesses for the six parameters G, n, m, Q_c, ϕ, and ω_f, the IMSL nonlinear regression routine DRNLIN is used to fit the creep data to the creep strain equation 14. This curve fitting requires that the creep strain and the corresponding time, stress, temperature, and time to failure for tensile creep specimens be available. This step of the parameter estimation methodology should ultimately result in convergence for the six CDM parameters stated above.

3) Finally, nonlinear regression is applied to equation 9 in order to obtain the last three parameters C, x, and Q_D. Note that this equation describes the time to failure as a function of stress and temperature, and thus uses one data point per creep curve. This data point obviously corresponds to that at the point of rupture. Equation 9 contains the already determined parameters m, ϕ, and ω_f. Therefore, these parameters are used as known constants for this procedure.

Due to the relatively few number of constants to be determined in this step (C, x, and Q_D), the nonlinear regression routine associated with reasonable starting guesses for these parameters is generally stable. In order to assure convergence and automate the process, the following procedure for choosing starting values for these three parameters is suggested. First, the parameters C and x are set equal to 1. Subsequently, these initial guesses for C, and x, and the already known values for m, ϕ, and ω_f in association with any creep rupture data point (t_f, σ, T) are substituted into equation 9 to compute a corresponding starting guess for Q_D. Now, the nonlinear regression procedure is applied to equation 9, using these three starting guesses for C, x, and Q_D. This results in convergence to a set of parameters corresponding to minimized SSE.

To test the methodology described above and make sure that different users would obtain the same results, two of the authors of this paper applied this procedure, independently from each other, to three different sets of actual creep data. Two of these creep data sets will be presented in the next section. They both converged to the same parameters, which proved to describe the creep curves well.

EXAMPLES

Two Benchmark examples of creep life prediction for ceramic components under multiaxial and uniaxial loading conditions are presented in this section to validate the CDM based approach and the CARES/Creep program. The first example is a silicon nitride NCX-5100 notched tensile specimen, which was analyzed as a part of Saint-Gobain/Norton advanced heat engines applications program. A multiaxial stress state exists at the notch root where creep rupture is predicted to occur. Hence, this example represents the application of the theory presented in this paper to multiaxial stress conditions. The second example involves the application of the theory to uniaxial tensile SN88 silicon nitride specimens. This example is used to demonstrate the ability of the CDM theory in representing the creep curves for materials displaying tertiary creep behavior.

Notched NCX-5100 Tensile Specimen

The aim of this example is to predict the multiaxial creep rupture behavior of silicon nitride NCX-5100, using creep data obtained from testing uniaxial smooth tensile specimens. All experimental creep data used in this example were obtained from reports published by Sundberg et al. (1994), Wade et al. (1994), and White et al. (1995). These creep data were part of a study on the joining of silicon nitride to silicon nitride for advanced heat engine applications. The Creep tests were conducted on two types of specimens. First, smooth tensile specimens were tested under creep conditions to characterize the creep response of the NCX-5100 material. Second, experiments on notched tensile bars were performed. This specimen configuration yields a multiaxial stress state in the vicinity of the notch root, where creep rupture is expected to initiate.

The uniaxial smooth tensile test geometry consists of a flat dog-bone specimen with tapered holes to account for the relief of out-of-plane alignment. The creep characteristics of the NCX-5100 silicon nitride material when isothermally loaded in uniaxial tension at temperatures in the 1275-1425°C range were investigated. The creep curves corresponding to these tests were provided to the authors for analysis.

Using the parameter estimation methodology described above, the nine CDM parameters were computed to be: G = 5944, n = 1.53, m = -0.422, Q_c/R = 41300, ω_f = 0.048, ϕ = 1.53, C = 0.347×10^{-5}, x = 2.83, and Q_D/R = 137600. These parameters are based on units of MPa, hours, and °K. The initial guesses for G, n, m, and Q_c/R when running the nonlinear regression routine, were obtained from the Baily-Norton model using the existing CARES/Creep multiple linear regression parameter estimation module. These parameters were found to be C_1 = 3211, C_2 = 1.3, C_3 = -0.374, and C_4 = 38700. The NCX-5100 material displays no tertiary creep behavior, which explains why ω_f is so small. Interestingly, the value ω_f= 4.8% is very close to a measurement of 5.5%, conducted by Menon et al. (1994) using image analysis, of the fraction of cavitated area after creep rupture of an NT-154 silicon nitride tensile specimen tested at 1400 °C. The NT-154 material also displays no tertiary creep behavior.

Figure 2 shows a comparison between experimental and analytical creep curves for smooth tensile NCX-5100 material. The analytical creep curve was calculated using equation 14. As can be seen from the figure, the CDM constitutive creep model was successful in describing the creep behavior for the NCX-5100 material.

The FEM mesh for the notched specimen is shown in Figure 3. Due to symmetry, analysis can be performed using one-quarter of the bar. The ANSYS model contains 598 axisymmetric elements (PLANE82). The notch is on the outside of the bar and its radius is 20% of the radius of the tensile specimen gage section. The mesh is refined near the notch root so that the stress state in that region can be more accurately characterized. The nonlinear transient creep FEM stress results obtained by the authors were very close to those reported by Foley et al. (1992) and White et al. (1995), thus yielding confidence in the FEM creep stress analysis performed in both studies.

Four notched bars were tested at 1370°C (Sundberg, et al., 1994). The reduced section average stresses were 105, 120, 135, and 150 MPa. Table 1 compares the experimental and predicted lives for these specimens as a function of their reduced section stress. As can be seen from the table, the predicted lives for these specimens using the CDM methodology described in this paper and computed via CARES/Creep compare well with the experimental failure times

Table 1. Predicted and experimental creep rupture results for the notched tensile creep specimens tested at 1370°C.

Reduced section average stress (MPa)	Experimental failure time (hour)	Predicted failure using CDM (hours)
105	314	94
120	44	47
135	39	25
150	3.5	13.5

The maximum principal stress distributions for the 120 MPa reduced average section stress specimen, as a function of time, are shown in Figure 4. Figures 4a, and 4b are the maximum principal stresses at 0 and 50 hours, respectively. A multiaxial stress state exists in the vicinity of the notch root, which reduces to a uniaxial stress state away from the notch. When the load is initially applied at time=0, the maximum principal stress at the notch root is computed to be 258 MPa. As time progresses (Figure 5) the stress relaxes at the notch root due to creep deformation, and decays to approximately 209 MPa after 50 hours. It is expected that given enough time, the maximum stress location would displace to the interior of the specimen. In a previous study conducted by the authors (Powers, et al., 1996) and based on steady state creep analysis using the Norton's model, it was found that at the time of failure the location of the maximum principal stress was a short distance within the specimen from the notch root. That finding concurred with that of White et al. (1995) who conducted similar steady state analysis. Stress relaxation directly influences damage calculations, and thus the predicted time and location of creep rupture. This is because the location of the maximum cumulative damage could displace as the stress redistributes with time. In the current study, which takes into account the primary creep effect and is based on CDM, the locations of both the maximum tensile stress and the maximum cumulative damage were at the notch root. This prediction concurs with fractographic examinations (White, et al., 1995) conducted on the failed notched specimens and found them all to have failed at the surface of the notch root. Figure 6 shows a cumulative damage map for the 120 MPa bar after 50 hours. Figure 7 displays the evolution of damage as a function of time at the notch root where rupture is predicted to occur. It can be seen from figures 6 and 7 that the damage reaches unity after 44 hours, which corresponds to rupture, at the notch root.

The maximum principal stress rather than the equivalent stress was used to predict the creep rupture life for the notched specimens. This was done, based on the discussion advanced in the multiaxial stress section of this paper, since the maximum principal stress resulted in the most conservative estimate for the creep rupture life (shorter life).

Smooth SN88 Tensile Specimen

This example is used to demonstrate the capability of the CDM model in capturing the tertiary creep behavior for isothermal constant stress tensile ceramic specimens. The SN88 silicon nitride material (NGK insulators, Nagoya, Japan) was selected for this purpose because it displays tertiary creep behavior, and because some of the data was available in the open literature (Luecke, et al., 1997, French, et al., 1996). The full data corresponding to the entire creep curves were supplied to the authors by Luecke. Five different laboratories were involved in testing a total of 24, 76-mm long SN88 tensile creep specimens at 1400°C under a 150 MPa stress.

The CDM equations presented in this paper thus far, were derived taking into account temperature and stress dependence. In other words, in order to compute the parameters in these equations, several creep tests conducted at various temperature and stress levels should be performed. Often, it is required to fit constitutive equations to isothermal constant stress creep curves such as in this example. Therefore, the CDM equations presented above should be reformulated to describe the creep behavior of specimens tested at the same temperature and stress levels. These isothermal and constant stress CDM equations are described next.

Since the stress and temperature in equation 7 are constant, then that equation describing the damage rate can be rewritten as:

$$\dot{\omega} = A\, t^{m}\,(1-\omega(t))^{-\phi} \qquad (24)$$

Where A, m, and ϕ are material constants. Note that the stress and temperature terms were incorporated into the A constant. Upon integration of equation 24 from t=0 to $t=t_f$, the following formula describing the time to failure is obtained:

$$t_f = \left\{ \frac{(1+m)}{A(1+\phi)} \left[1-(1-\omega_f)^{1+\phi} \right] \right\}^{\frac{1}{1+m}} \qquad (25)$$

Inversely, equation 25 can be rewritten in terms of the critical damage at failure, ω_f, as:

$$\omega_f = 1-\left[1-\frac{A(1+\phi)\, t_f^{1+m}}{(1+m)} \right]^{\frac{1}{1+\phi}} \qquad (26)$$

The damage at a given time t can be obtained by replacing t_f with t in equation 26:

$$\omega(t) = 1-\left[1-\frac{A(1+\phi)\, t^{1+m}}{(1+m)} \right]^{\frac{1}{1+\phi}} \qquad (27)$$

Combining equations 26 and 27, yields the following alternative form for $\omega(t)$:

$$\omega(t) = 1-\left\{ 1-\left(\frac{t}{t_f} \right)^{1+m} \left[1-(1-\omega_f)^{1+\phi} \right] \right\}^{\frac{1}{1+\phi}} \qquad (28)$$

The creep rate equation 8, can be restated for isothermal and constant stress condition in the following form:

$$\dot{\varepsilon} = B\, t^{m}\,(1-\omega(t))^{-n} \qquad (29)$$

Substituting equation 28 into equation 29, yields the following function for the creep rate:

$$\dot{\varepsilon} = B t^{m} \left\{ 1-\left(\frac{t}{t_f} \right)^{1+m} \left[1-(1-\omega_f)^{1+\phi} \right] \right\}^{\frac{-n}{1+\phi}} \qquad (30)$$

Integrating equation 30 results in the following equation describing the creep strain as a function of time:

$$\varepsilon(t) = \frac{B\, t_f^{1+m}}{(1+m)\left(\frac{1+\phi-n}{1+\phi} \right)\left[1-(1-\omega_f)^{1+\phi} \right]} \left\{ 1-\left[1-\left(\frac{t}{t_f} \right)^{1+m} \left[1-(1-\omega_f)^{1+\phi} \right] \right]^{\frac{1+\phi-n}{1+\phi}} \right\} \qquad (31)$$

Combining equations 28 and 31, result in the following equation describing the creep strain as a function of the current state of damage:

$$\varepsilon(t)=\frac{B\,t_f^{1+m}}{(1+m)\left(\frac{1+\phi-n}{1+\phi}\right)\left[1-(1-\omega_f)^{1+\phi}\right]}\left\{1-\left[1-\omega(t)\right]^{1+\phi-n}\right\} \qquad (32)$$

Assuming that $\phi = n$, which implies that the damage accumulation affects the damage rate in a similar fashion as it affects the creep rate, equation 31 simplifies to the following form:

$$\varepsilon(t)=\frac{B(1+\phi)\,t_f^{1+m}}{(1+m)\left[1-(1-\omega_f)^{1+\phi}\right]}\left\{1-\left[1-\left(\frac{t}{t_f}\right)^{1+m}\left[1-(1-\omega_f)^{1+\phi}\right]\right]^{\frac{1}{1+\phi}}\right\} \qquad (33)$$

The assumption that $\phi = n$ is very reasonable based on nonlinear regression parameter estimation results. Note that for the NCX-5100 material, the parameters, n and ϕ, converged to the same value. The same result was found by the authors for the NT154 silicon nitride material, which is not shown in this paper.

The SN88 creep parameters were computed using the same parameter estimation methodology described previously. Nonlinear regression applied to equation 33 was used to determine the four parameters B, m, ϕ, and ω_f. They were found to be; B = 0.000838, m = -0.456, ϕ = 1878, and ω_f = 0.0007. Subsequently, equation 25 was regressed to obtain the last parameter A. It was calculated to be $A = 2.01\text{x}10^{-5}$. These values are based on units of hours.

Figure 8 shows the experimental creep curves for several SN88 tensile specimens tested at 1400°C under a 150 MPa stress. In addition, this Figure displays the corresponding predicted creep curve plotted using the creep parameters listed above. The X sign shown at the end of the predicted creep curve indicates the predicted time to failure for this specimen. It is obvious from Figure 8 that some scatter exists among the various creep curves. The predicted creep curve falls in the middle of the experimental creep curves and displays tertiary creep behavior. The predicted time to failure also compares very well with the measured rupture times (end of experimental creep curves). These results show that the CDM model described above is capable of representing entire creep curves including the tertiary creep regime.

The critical damage parameter, ω_f, was found to be low for the SN88 material even though it displays tertiary creep behavior. This is because the increase in the creep rate within the tertiary creep regime is a function of $(1-\omega)^{\phi}$, and thus the parameters ω and ϕ. Since the exponent ϕ was found to be a large number, this compensated for the low value computed for ω_f. The nonlinear regression routine through its iterative procedure converges to the optimum set of parameters that would minimize the SSE for the data set in question.

CONCLUSION

A creep life prediction methodology based on the continuum damage mechanics theory was described. In this theory, the uniaxial creep rate is described in terms of stress, temperature, time, and the current state of material damage. The damage rate is assumed to vary with stress, temperature, time, and the current state of damage itself. Multiaxial creep and creep rupture formulations of the CDM approach were presented. Parameter estimation methodologies based on nonlinear regression analysis were also described for both, isothermal constant stress states and anisothermal variable stress conditions. Several advantages are apparent to the creep rupture life methodology presented in this paper. First, this methodology yields a cumulative damage map for the component showing the critical locations where failure would originate. This capability is very helpful for practical design applications. Through viewing such a damage map, the user can change the design parameters to reduce the damage at the critical locations and optimize the design. In creep type loading applications, it is not a trivial task to predict the location of failure since the multiaxial stress components get redistributed as time elapses. Thus, failure will not necessarily occur at the location where stresses are highest at the beginning of loading or at the time of failure, but can take place elsewhere. Second, this methodology is capable of incorporating the effects of primary and tertiary creep on

rupture. Third, any equivalent stress criterion can be used to predict the component's life. Fourth and perhaps most importantly, this methodology takes into account the effect of instantaneous damage on the deformation and rupture of the component. This creep life prediction methodology was preliminarily added to the integrated design code CARES/Creep (Ceramics Analysis and Reliability Evaluation of Structures/Creep), which is a postprocessor program to commercially available finite element analysis (FEA) packages. Two examples, showing comparisons between experimental and predicted creep lives of ceramic specimens, were used to demonstrate the viability of this methodology and the CARES/Creep program.

REFERENCES

Dunne, F. P. E., Othamn, A. M., Hall, F. R., and hayhurst, L. M., 1990, "Representation of Uniaxial Creep Curves Using Continuum Damage Mechanics," *International Journal of mechanical Science*, Vol. 32, No. 11, pp. 945-957.

Ferber, M. K., and Jenkins, M. G., 1992, "Empirical Evaluation of Tensile Creep and Creep Rupture in a HIPed Silicon Nitride," in *Creep: Characterization, Damage and Life Assessment*, ASM International Woodford, D. A., Townley, C. H. A., and Ohnami, M., Eds., pp. 81-90.

Foley, M., Rossi, G., Sundberg, G., Wade, J., and Wu, F., 1992, "Analytical and Experimental Evaluation of Joining Silicon Carbide to Silicon Carbide and Silicon Nitride to Silicon Nitride for Heat Engine Applications," Final Report, Ceramic Technology for Advanced Heat Engines, Oak Ridge National Lab.

French, J. D., and Wiederhorn, S. M., 1996, "Tensile Specimens from Ceramic Components," *Journal of the American Ceramic Society*, Vol. 79, No. 2, pp. 550-552.

Hales, R., 1988, "Physical Mechanisms of Fracture in Combined Creep and Fracture," *Proceedings Inst Metals Conference on materials and Engineering Design*, London.

Hault, Jan, 1987, "Introduction and General Overview," *Continuum Damage Mechanics Theory and Applications*, Krajcinovic, D., and Lemaitre, J., Eds., Springer-Verlag, New York.

Hayhurst, D. R., Dimmer, P. R., and Cheruka, M. W., 1975, "Estimates of the Creep Rupture Lifetime of Structures Using the finite Element method," *Journal of Mechanical Physics of Solids*, Vol. 23, pp. 335-355.

Hayhurst, L. M., Dimmer, P. R., and Morrison, C. J., 1984a, "Development of Continuum Damage in the Creep Rupture of Notched Bars," *Phil. Trans. R. Soc. Lond.*, Vol. 311, pp. 103-129.

Hayhurst, L. M., Brown, P. R., and Morrison, C. J., 1984b, "The Role of Continuum Damage in Creep Crack Growth," *Phil. Trans. R. Soc. Lond.*, Vol. 311, pp. 131-158.

Hazime, R. M., and White, C. S., 1996,"An Internal Variable , Creep Damage Model of a Silicon Nitride," submitted for publication in *Materials Science and Engineering*.

Jadaan, O. M., Powers, L. M., and Gyekenyesi, J. P., 1997, "Creep Life Prediction of Ceramic Components Subjected to Transient Tensile and Compressive Stress States," ASME paper 97-GT-319.

Kachanov, L. M., 1958, "On Creep Rupture Time," Izv. Acad. Nauk SSSR, Otd. Tech. Nauk, No. 8.

Kachanov, L. M., 1986, *Introduction to Continuum Damage mechanics*, MartinusNijhof, Boston.

Leckie, F. A., Hayhurst, L. M., 1977, "Constitutive Equations for Creep Rupture," *Acta Metallurgica*, Vol. 25, pp. 1059-1070.

Luecke, W. E., and Wiederhorn, S. M., 1997, "Interlaboratory Verification of Silicon Nitride Tensile Creep properties," *Journal of the American Ceramic Society*, Vol. 80, No. 4, pp. 831-838.

Menon, M., Fang, H., Wu, D., Jenkins, M., and Ferber, M., 1994, "Creep and Stress Rupture Behavior of an Advanced Silicon Nitride: Part III, Stress Rupture and Monkman-Grant Relationships," *Journal of the American Ceramic Society*, Vol. 77, pp. 1235-1241.

Monkman, F., and Grant N., 1956, "An Empirical Relationship Between Rupture Life and Minimum Creep rate in Creep-Rupture Test," *Proceedings of the American Society for Testing and materials*, Vol. 56, pp. 593-620.

Othman, A. M., and hayhurst, L. M., 1990, "Multi-Axial Creep Rupture of a Model Structure Using a two parameter material Model," *International Journal of mechanical Science*, Vol. 32, No. 1, pp. 35-48.

Penny, R. K., and Marriott, D. L., 1995, *Design for Creep*, Chapman & hall, London.

Powers, L. M., Jadaan, O. M., and Gyekenyesi, J. P., 1996, "Creep Life of Ceramic Components Using a Finite Element Based Integrated Design Program (CARES/Creep)," ASME paper 96-GT-369.

Press, W. H., Flannery, B. P., Teukolsky, S. A., and Vetterling, 1989, *Numerical Recipes*, Cambridge University Press, Cambridge.

Rabotonov, Yu. N., 1969, *Creep Problems in Structural members*, North-Holland, Amsterdam.

Robinson, E. L., 1952, "Effect of temperature Variation on the Long-Time Rupture Strength of Steels," *Trans. ASME 74*, pp. 777-780.

Stamm, H., and von Estroff, U., 1992,"Determination of Creep Damage in Steels ," *Proceedings 5th International Conference on Creep of Materials*, Florida, USA.

Sundberg, G., Vartabedian, A., Wade, J., and White, C., 1994, "Analytical and Experimental Evaluation of Joining Silicon Carbide to Silicon Carbide and Silicon Nitride to Silicon Nitride for Advanced Heat Engine Applications Phase II," Final Report, Ceramic Technology Project, Oak Ridge National Lab.

Todd, J. A., and Xu, A.-Y., 1989, "The High Temperature Creep Deformation of Si_3N4-$6Y_2O_3$-$2Al_2O_3$," *Journal of materials Science*, Vol. 24, pp. 4443-4452.

Miner, M. A., 1945, "Cumulative Damage in fatigue," *Journal of Applied Mechanics*, Vol. 12, pp. A159-A164.

Wade, J., White, C., and Wu, F., 1994, "Predicting Creep Behavior of Silicon Nitride Components Using Finite Element Techniques," in *Life Prediction Methodologies and Data for Ceramic Materials*, ASTM STP 1201, Brinkman, C., and Duffy, S., Eds., American Society for Testing and materials, Philadelphia, pp. 360-372.

White, C., Vartabedian, A., Wade, J., and Tracey, D., 1995, "Notched Tensile Creep Testing of Ceramics," *Materials Science and Engineering*, A203, 217-221.

Wiederhorn, S., Quinn, G., and Krause, R., 1994, "Fracture Mechanism Maps: Their Applicability to Silicon Nitride," *Life Prediction Methodologies and Data for Ceramic materials*, ASTM STP-1201, Brinkman, C. R., and Duffy, S. F., eds., American Society for Testing and materials, Philadelphia, pp. 36-61.

Zamrik, S. Y., and Davis, D. C., 1990, "A Ductility Exhaustion Approach for Axial fatigue-Creep Damage Assessment Using Type 316 Stainless Steel," ASME PVP, 215.

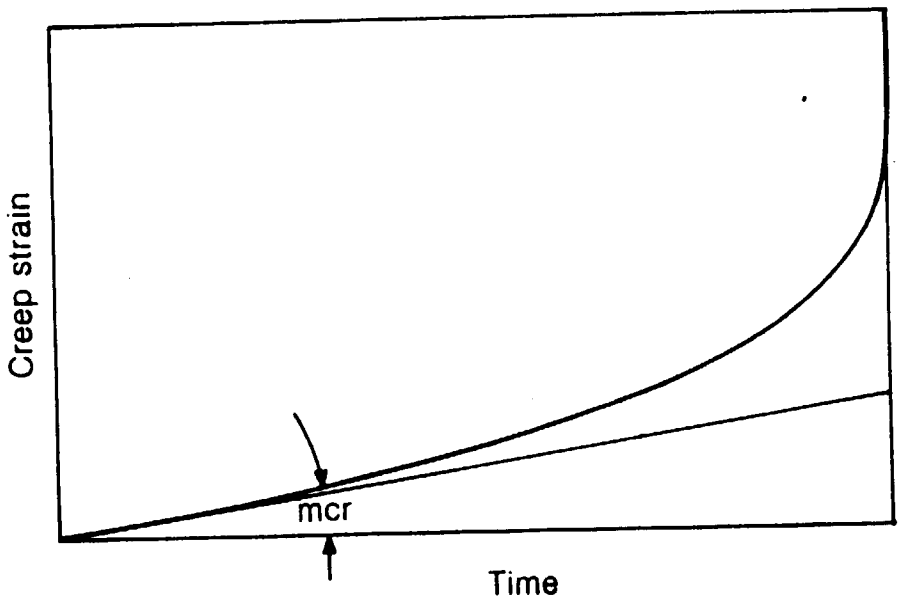

Fig 1. Schematic creep curve representation using Kachanov'sCDM model (equations 5 and 6).

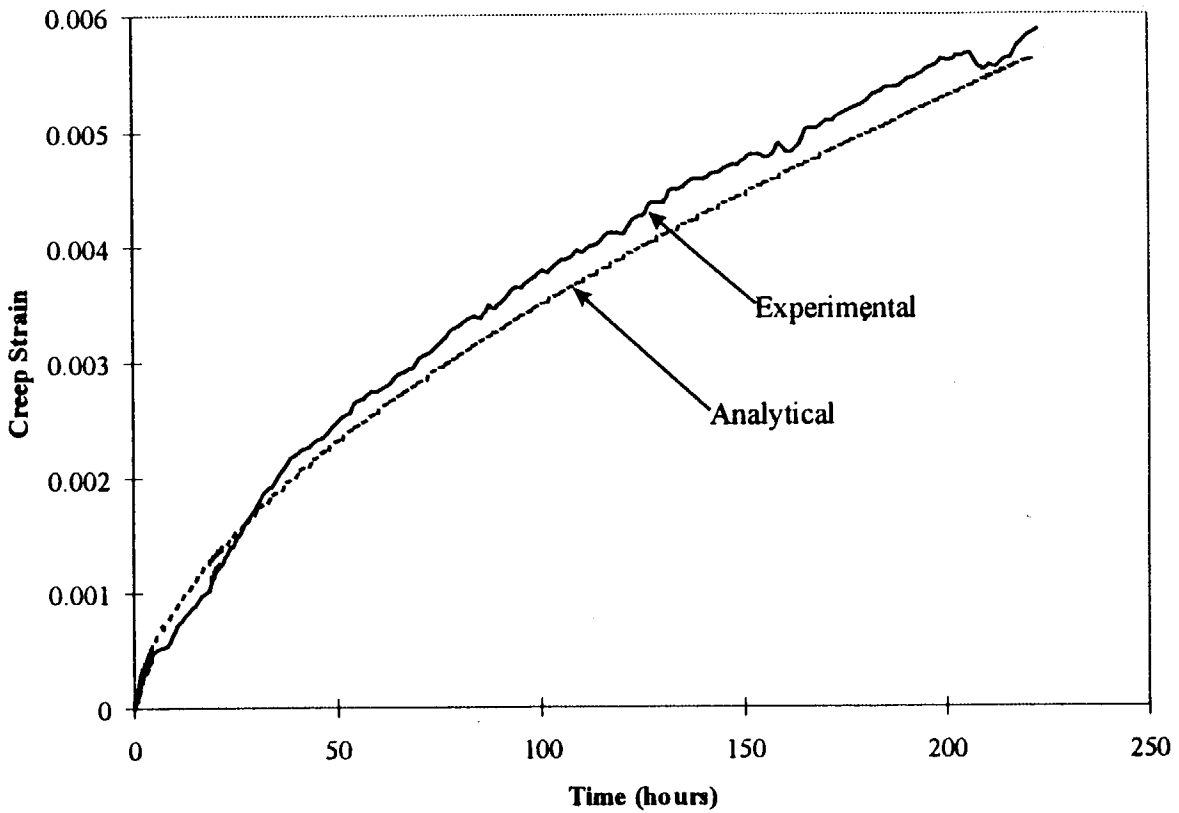

Fig 2. Comparison between experimental and analytical creep curves for the NCX-5100 material at 1350°C and 175 MPa.

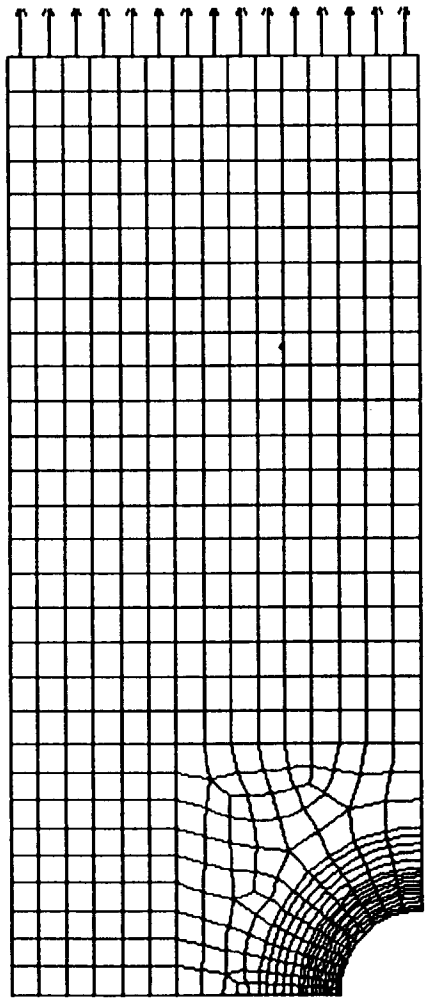

Fig 3. Axisymmetric finite element mesh for the notched specimen.

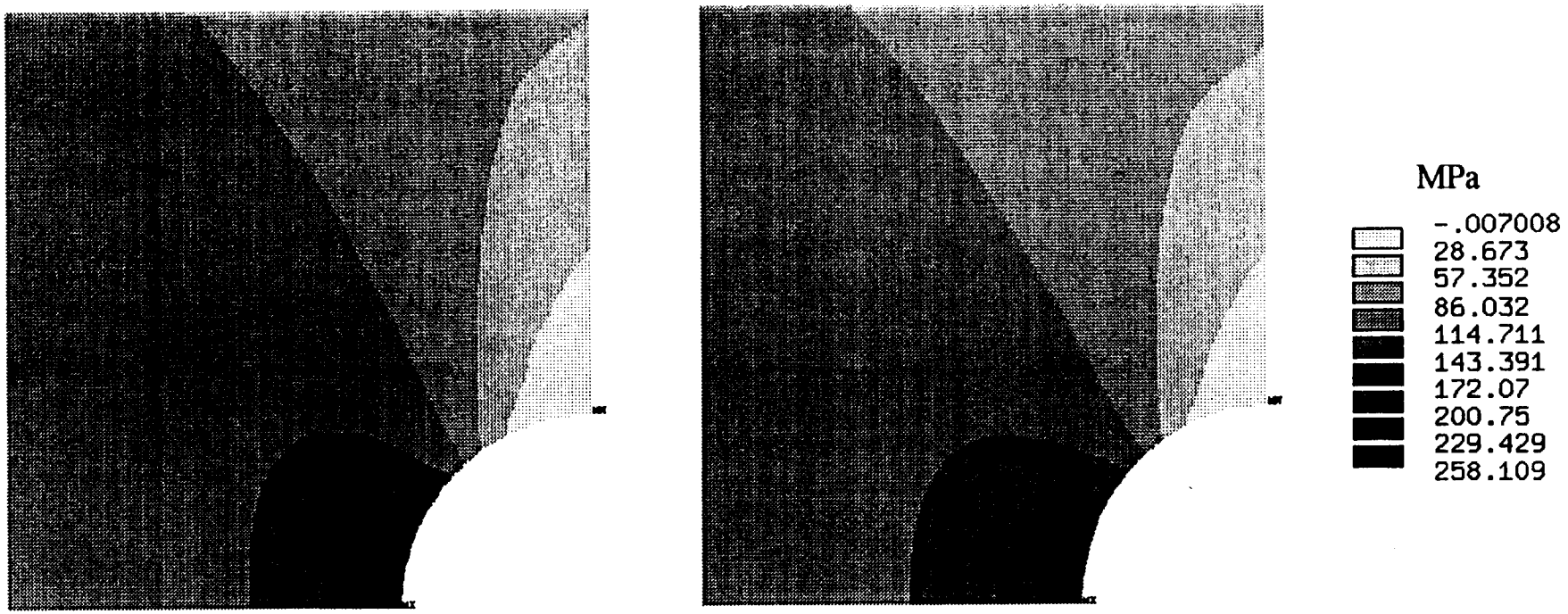

a)

b)

Fig 4. Maximum principal stress in the notched tensile specimen tested at a reduced section stress of 120 MPa at time equal to a) zero and b) 50 hours.

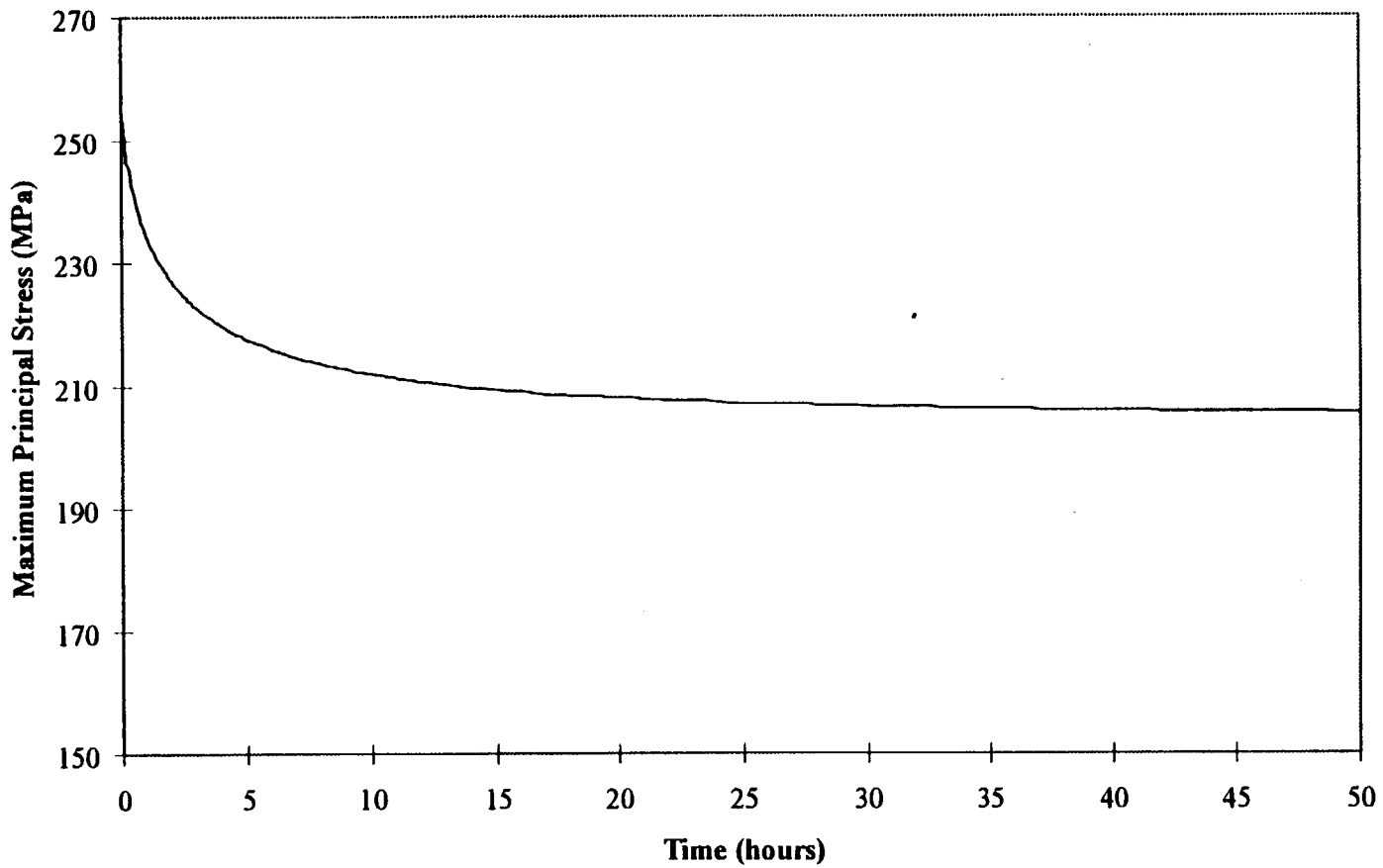

Fig 5. Maximum principal stress relaxation at the notch root for the NCX-5100 specimen tested at a reduced section stress of 120 MPa.

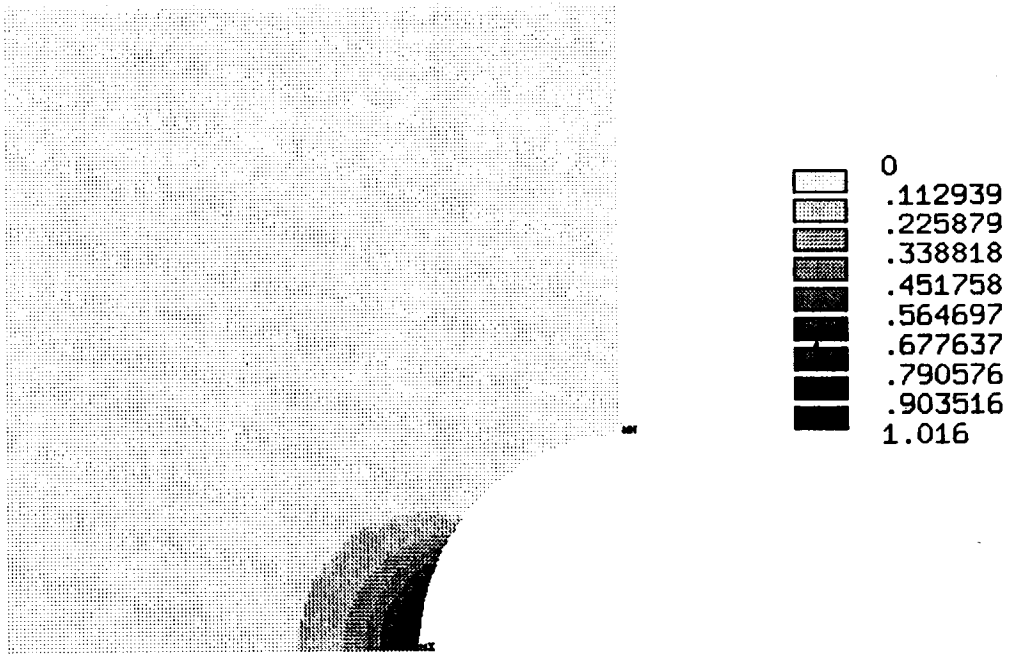

Fig 6. Cumulative damage distribution in the notched tensile specimen tested at a reduced section stress of 120 Mpa.

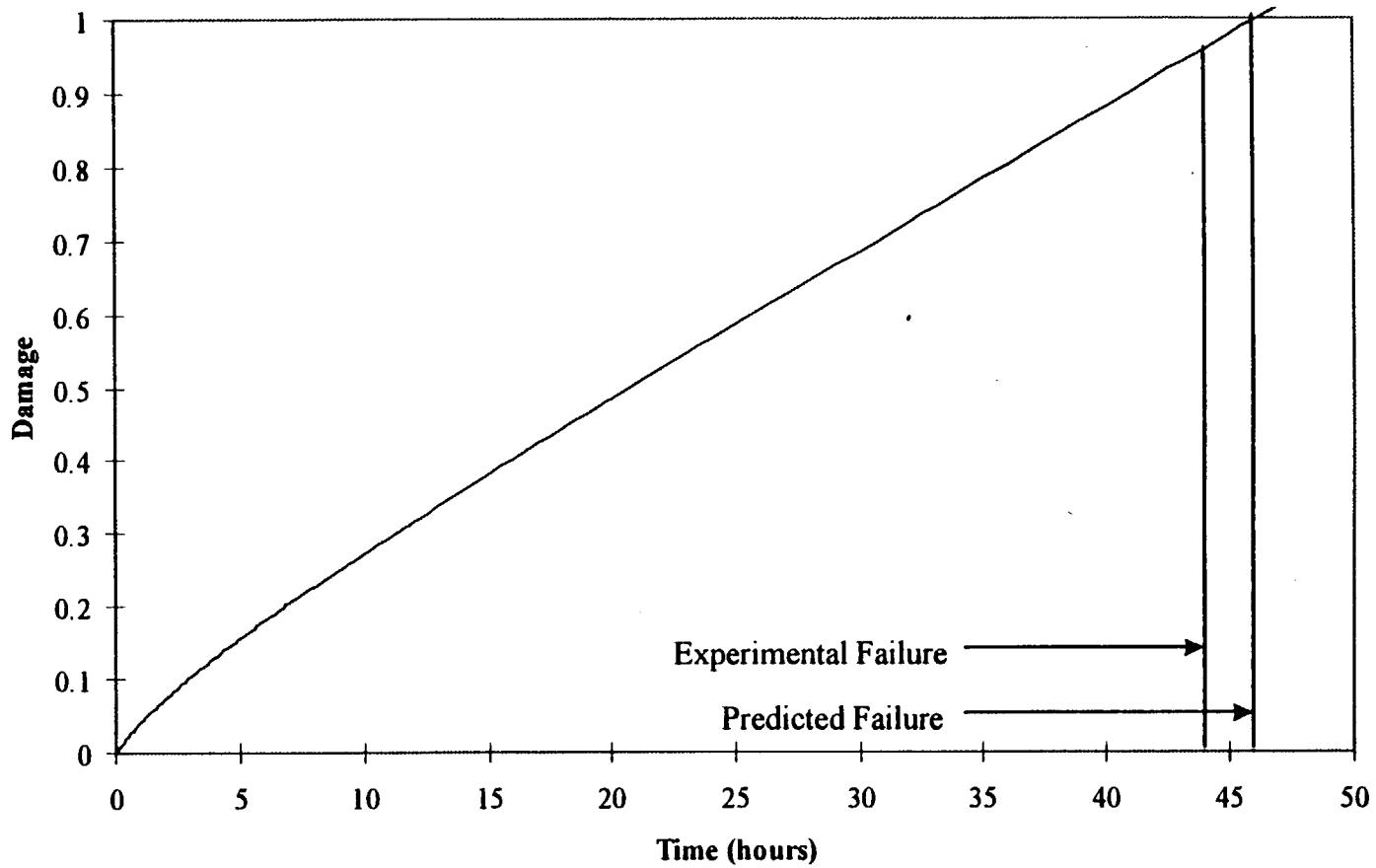

Fig 7 Evolution of damage as a function of time at the notch root of the tensile specimen tested at a reduced section stress of 120 MPa.

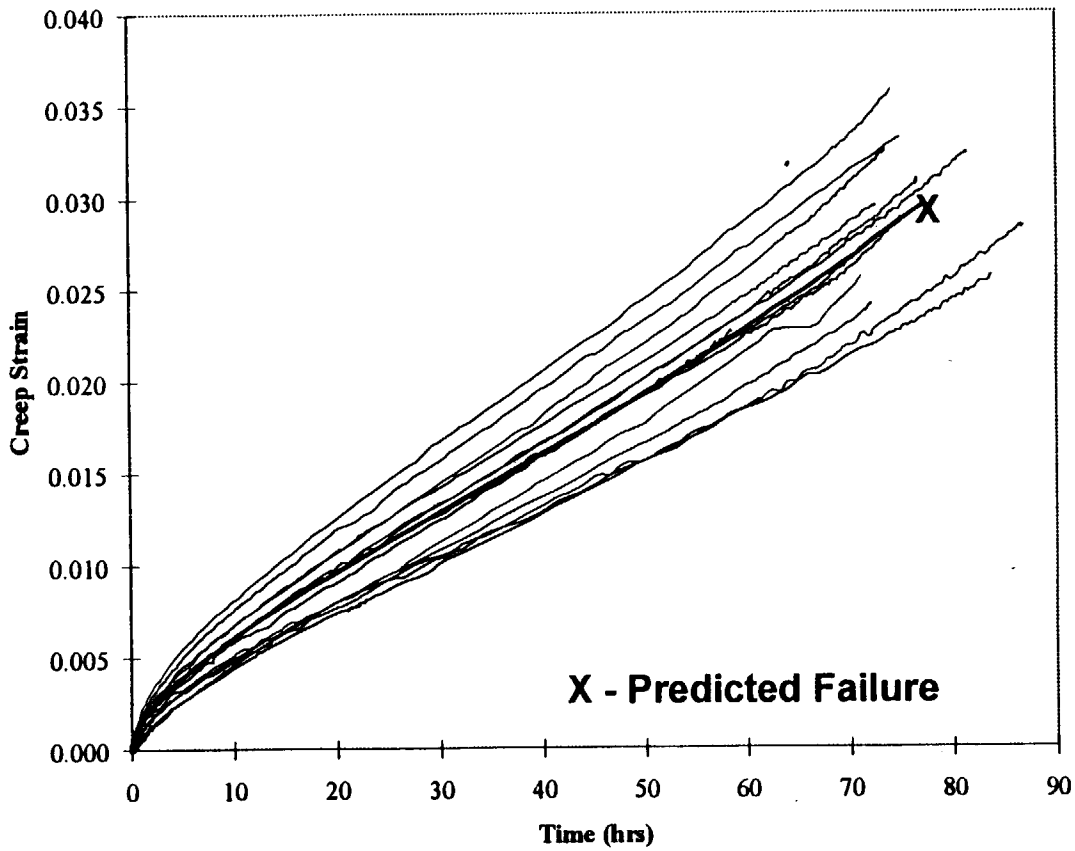

Fig 8. Comparison between experimental and analytical creep curves for the SN88 material.